Discharge and suspended sediment dynamics in an Indian Himalayan river system

ABSTRACT (200 wds)

KEY WORDS: suspended sediment dynamics; discharge; Himalayas; Ladakh

by

Tim Stott[1] & Anne-Marie Nuttall[2]

[1] Faculty of Education, Health & Community, Liverpool John Moores University, UK.

[2]Geography School, University of the Highlands and Islands, Scotland, UK.

Prof Tim Stott

Faculty of Education, Health & Community,

Liverpool John Moores University,

I.M. Marsh Campus,

Barkhill Road,

Liverpool L17 6BD

UK.

Email: t.a.stott@ljmu.ac.uk

Tel: +44 (0) 151 231 5329

Dr Anne-Marie Nuttall,

Geography School,

University of the Highlands and Islands,

3 Longman Road, Longman South, Inverness IV1 1SA,

Scotland, UK.

Email: anne-marie.nuttall@uhi.ac.uk

BACKGROUND

A pure, clean and reliable water supply is of paramount importance in India where meeting the requirements of a rising population is one of the big challenges of the 21st century. Climate change in the Indian subcontinent, identified by the Intergovernmental Panel on Climate Change (IPCC, 2013) as the region with the highest level of climate instability, is of major concern (Immerzeel *et al.,* 2010; Morton, 2011). In 2010 the floods in the Indus basin were the worst in history (Hobley *et al.,* 2012). Two thousand people died in Pakistan and in the high-altitude desert of Ladakh, intense rain and floods centred around Leh, washed away homes and villages and killed 200 people. At present, 10 % of the earth's land-mass is covered with snow. Of this total area, 84.16 % is in the Antarctic, 13.9 % in Greenland, 0.77 % in the Himalaya, 0.51 % in North America, 0.37 % in Africa, 0.15 % in South America, and 0.06 % in Europe. Outside the Polar Regions, the Himalaya has the maximum concentration of glaciers – 9.04 % of its area. An additional 30-to-40 % is covered with snow. The glaciers of the Himalaya are the Third Pole (Dyhrenfurth, 2011). They feed the giant rivers of Asia, support half of humanity and can have a significant influence on regional water availability (Immerzeel *et al.,* 2009). Recent studies have confirmed the important role of high mountain areas of the world as sources of freshwater for the population living in the adjacent lowlands (eg. Bandyopadhyay *et al.,* 1997; Viviroli &Weingartner, 2004; Barnett *et al.,* 2005; Viviroli *et al.,* 2007; Thayyen & Gergan, 2010)

Despite the hydrological importance of glaciers for the adjoining lowlands, data on the glaciers of the Himalaya, Karakorum, and Hindu Kush ranges are sparse and inconsistent. There is a lack of long-term series and field investigations, especially for glaciers at higher altitudes (Armstrong, 2010; Schmidt & Nüsser, 2012).

AIMS

This study aimed to monitor river discharge and suspended sediment concentration during the melt season to assess discharge and suspended sediment dynamics in the Zara river which is likely to be a future focus for a water abstraction scheme for the local population and that of Debring in the neighbouring valley.

STUDY AREA

Ladakh straddles the boundary zone between the Eurasian continent and the Indian sub-continent (Fig. 1). The Indus Valley is located just north of the so-called suture zone, where two continental plates collided some 50 million years ago. North and south of the Indus are a series of mountain ranges, more or less parallel to the Indus valley known as the Great Himalayan range that marks the southwestern boundary; the Zanskar Range – mountains formed of oceanic sediments – between the Great Himalayas and the Indus; the Ladakh Range – mountains formed of plutonic rocks – north of the Indus; and the Karakoram that marks the

northern boundary. Ladakh is a high-altitude desert region in the northwest Indian Himalaya (Fig. 1). Leh, the main town in the region, receives only 80–100 mm of rain in a typical year (Spate *et al.,* 1976); average rainfall in August is 15.4 mm (India Meteorological Department, 2010).

This study was located some 80km due south of Leh on the Zara River on the east side of the Zanskar mountain range in Ladakh, latitude 33.451002°, longitude 77.773931°, altitude 4880m asl. The study catchment (Fig. 1) is 85 km^2 and contains 17 small (< 1km^2) glaciers which are confined to the 5400m-6000m altitude range. The total are covered by permanent ice during August (the time of this study) is 8.5km^2, meaning that the study catchment is 10% ice covered. Figs 2A and 2B show typical glaciers in the study catchment which exist between 5400 – 6000m altitude and are found only on NE slopes. Schmidt & Nüsser (2012) reported changes of small glaciers in the Trans-Himalayan Kang Yatze Massif, Ladakh, between 1969 and 2010 using satellite images to detect and analyze area changes of 121 small glaciers and to measure the retreat of 60 cirque and valley glaciers. Over the last four decades, the glaciated area decreased by about 14% (0.3%yr^{-1}) from 96.4 to 82.6 km^2 and the average ice front retreat amounts to 125 m (3 m yr^{-1}). The ice cover loss shows a high decadal variability with the maximum shrinkage between 1991 and 2002 (0.6%yr^{-1}), followed by a lower decrease rate since then (0.2%yr^{-1}). Given these estimates, it is likely that the glaciers in this study catchment are relatively stable.

Under 'normal' arid low flow conditions, flow in the Zara River is likely to be dominated by snow and glacial meltwater discharge fed from the 17 small glaciers in the highest elevations of the catchment (Fig. 1). Meltwater is likely to entrain fine sediment which is transported in suspension and Haritashya *et al*. (2006) found that maximum suspended sediment concentration (SSC) in meltwater from the Gangotri Glacier, Garhwal Himalaya, was observed in July followed by August, as did Hasnain & Thayyen (1999) for SSC in the waters draining from the Dokriani glacier. However, both these studies were based in the monsoon-dominated central part of the Himalaya so a study in the arid Himalayan region is needed.

Methods

A stage board, pressure transducer and Partech 0-750 mg/L turbidity sensor were installed at the side of the channel (Δ in Fig. 1, photograph in Fig. 2C) on 6 August 2013. Data were recorded by a Squirrel 2010 data logger at 2-min scan time until 23 August 2013. A rating relationship between pressure transducer voltage and stage was established (R^2 = 0.63, n = 25, $p<0.01$) to convert mV to stage. Discharge was measured on 7 occasions (Fig. 2D) using the velocity area method (Herschey, 1978) with depth, and velocity at 0.6 depth, recorded at 0.5m intervals across the 9.75m wide channel. The stage-discharge rating relationship established (Fig. 3A) was used to convert the 2-min stage record into discharge for the 23 day study period. Daily site visits were made to retrieve 1 litre manual water samples which were filtered on-site and later gravimetrically analysed for their suspended sediment concentration (SSC). The measured SSCs were used to calibrate the turbidity record (Fig. 3B). Air temperature was

measured by a shaded TinyTag Plus data logger (Fig. 2C) at 5-min intervals and rainfall was recorded at daily 09.00 AM local time by a ground level rain gauge.

Fig. 2 here

Fig. 3 here

RESULTS

Ai temperature varied diurnally between 4.3 ^{o}C and 25.9 ^{o}C with a mean of 13.8 ^{o}C (Fig. 4A). Rain was recorded on 11 of the 17 days of the study period with significant amounts recorded on the 7th August (8.4 mm), 12th August (12.7 mm) and 17th of August (12.7 mm), (Fig. 4B). A total of 34.9 mm fell over the 17 day study period which would seem to be unusual for this high altitude desert, given that Leh, the main town in the region (80 km to the north), receives only 80–100 mm of rain in a typical year (Spate *et al.,* 1976) and average rainfall in August is 15.4 mm (India Meteorological Department, 2010). On most occasions when rain fell at the river monitoring station at an altitude of 4850m, snow was observed on the surrounding mountains.

Fig. 4 here

Q ranged between 0.4 and 5.3 m^3/s, and the mean for the period was 1.2 m^3/s. SSC measured in 63 manual samples ranged from 5 to 92 mg/L, and the mean SSC was 17 mg/L. When the SSC v Tu calibration relationship (Fig. 3B) was applied to the 2-min turbidity data the predicted SSC for the study is plotted along with Q in Fig. 5. The mean predicted SSC was 21.3 mg/L which agrees well with the measured value of 17 mg/L from the 62 samples, and the maximum predicted SSC was 91.0 mg/L which agrees well the highest sampled value of 92.1 mg/L.

Fig. 5 here

A clear diurnal pattern is observed in both Q and SSC. This pattern most likely reflects snow and glacier melt from 17 glaciers which supply melt water to the Zara river. Melt is driven by air temperature, although rainfall occasionally modified the observed Q.

DISCUSSION

Lag times

Table 1 presents a simple analysis of daily data. Air temperature (T_{air}) peaked between 08:55 and 17:50 with the average time being 13:32 (early afternoon), whereas river peak discharge (Q_{peak}) was between 10:05 and 16:39 with the mean being 12:26. The calculated lag times between T_{air} and Q_{peak} ranged between +05:35 (ie. peak T_{air} was 5 h 35 min before Q_{peak}) and –

02:49 (ie. peak T_{air} was 2 h 49 min after Q_{peak}). T_{air} peaked after Q_{peak} on 4 of the 16 days while Q_{peak} was after peak T_{air} on 12 of the 16 days. From the 147 velocity measurements taken at the monitoring cross-section over the study period, the mean velocity was 0.92 m/s or 3.3 km/h. As can be seen from Fig. 1, some of the most distant glaciers from the river monitoring station are 12 km away. At a speed of 3.3 km/h it would take melt water approximately 4 h to reach the monitoring station.

As can be seen from Fig. 4B and the final column in Table 1, rainfall was recorded on 11 of the 16 complete days in the analysis, though significant rain fell on only three days: 07-Aug (8.4mm), 12-Aug (12.7mm) and 17-Aug (12.7mm). The 8.4 mm which fell on 07-Aug resulted in a higher Q_{peak} of 4.1 m^3/s the following day on 08-Aug and the 12.7mm which fell on 12-Aug pushed the Q_{peak} up from 0.5 m to 2 m^3/s on 13-Aug. However, 12.7mm of rain falling on 17-Aug caused only a slight increase in Q_{peak} the next day from 1 to 2.3 m^3/s (18-Aug), but there was the most significant increase in Q_{peak} from 0.5 to 5.1 m^3/s on 19-Aug and to 4.8 m^3/s on 20-Aug. Given that minimum air temperatures at the monitoring station were around 4-5 ^oC, with and environmental lapse rate of say 0.6 $^oC/100m$, it is likely that temperatures on the surrounding mountain tops (up to 1000 m higher) would be around 6 ^oC cooler, i.e. below freezing, so that precipitation falling above 5600m was falling as snow. The exceptionally high Q_{peak} on 19 and 20-Aug would have been caused by snow at higher elevations melting.

Table 1 here

Suspended Sediment Dynamics

The SSCs observed in the study are low on a global scale, and certainly for the Himalayan region (Hasnain *et al.,* 1989; Hasnain, 1992), where tectonic uplift and lack of vegetation cover tend to result in some of the world's highest suspended sediment yields (Walling & Fang, 2003). SSCs measured in this study compare closely with those measured in a similar undisturbed catchment in SW Greenland (Stott *et al.,* 2014) where the mean SSC was 23 mg/L. Along with T_{air}, Q_{peak} and lag times, suspended sediment concentration peaks (SSC_{peak}), times of peak and lag times with Q_{peak} are also presented in Table 1. The highest SSC peaks were on days which coincide with the highest Q peaks, i.e. 08-Aug; 13-Aug and 19-22 Aug inclusive. It is probable that during high discharge events the river rises and as it does, it entrains fine sediment from its banks and transports this downstream until Q falls and the river banks no longer supply sediment so the SSC falls again. Table 1 also shows that Q_{peak} – SSC_{peak} lag times range from +05:48 (i.e. Q_{peak} is 5 h 48 min before SSC_{peak}) to -04:22 (where Q_{peak} is 4 h 22 min after SSC_{peak}). However, these are extremes and the mean Q_{peak} – SSC_{peak} lag time is only +50 mins.

Fig. 6 shows the daily Q and SSC time series plots which reveal the detailed dynamics of this relationship.

Fig. 6 here

Two observations on these Q and SSC time series plots are worthy of mention. First, there are examples of hysteresis. Hysteresis is where the Q and SSC peak are out of phase, i.e. one peaks before the other. When Q peaks before SSC the hysteresis is said to be clockwise, whereas when SSC peaks before Q it is anticlockwise. The penultimate column in Table 1 indicates where there is hysteresis in the Q and SSC patterns and whether it is clockwise of anticlockwise. Clockwise hysteresis occurred on 8, 9, 10, 15, 19, 20 and 22 August when Q peaked before SSC, whereas anticlockwise hysteresis occurred on 7, 11, 12, 16, 17 and 18 August and no hysteresis was observed on 13, 14 and 21 August. The second observation to be noted is that of sediment exhaustion. On several days the Q and SSC peaked, but on the falling limb of the hydrograph the Q rose again (eg. 16, 17, 18 August) but the SSC did not rise again in response to the increased Q. These are examples of SSC exhaustion, when the supply of SSC (most probably from banks) is used up and so further increases in Q do not result in higher SSCs. Figure 7 plots SSC predicted from the turbidity records (as used in Figs. 6 and 6), but also plots SSC predicted from the Q v SSC rating relationship (Fig. 3C). For each day of the study, the difference between the SSC predicted from the turbidity records and the SSC predicted from the Q v SSC rating relationship is calculated from the time of the SSC peak (usually between 11:00 and 13:00 and midnight. If this difference is negative (i.e. the SSC predicted from the turbidity records is lower than SSC predicted from the Q v SSC rating relationship) then this is taken as a measure of the amount of suspended sediment exhaustion, and vice versa. This difference is plotted for each day of the study on the secondary (right hand) axis in Fig. 7.

Fig. 7 here

The plot indicates the changes in sediment exhaustion over the study, from a slightly negative balance from 7- 11 August to a positive difference on 13 and 13th to a sudden swing to highly negative on 15th to 18th then a return to a net positive balance on 19 – 20th decreasing into negative balance for 21st and 22nd. An explanation for these changes in sediment availability is not obvious. While there was significant rainfall on 7th, 12th and 17th August, this does not appear to explain these changes. It could be that the rainfall on 17th August fell as snow at higher elevations and the subsequent increases in Q due to snowmelt on 19th and 20th August in particular, brought an increased suspended sediment load due to freeze-thaw processes high up on the mountainsides releasing fine sediment which was transported downstream by the increased melt water. These processes may also have been active in the first part of the study period (11-13th August). This same pattern is reflected in the daily suspended sediment loads for the study period (Fig. 8).

Implications for Water Management

Data such as these presented here could be useful for engineers and other parties interested in water abstraction for human consumption, agriculture or hydro-electricity generation purposes. Water which contains sediment in suspension needs to be treated by filtration or settling before consumption. Sediment in water entering hydro-electricity generating turbines causes damage to turbines by scouring. A more precise understanding of when Q and SSC are high in such

Himalayan river systems offers the possibility of abstracting pure, clean water when SSC is at its lowest (i.e. SSC is lowest generally between 15:00 and 10:00 the following morning). It appears that considerable efforts have already been made to abstract and divert water from the Zara river (some 2 km downstream from the study site shown in Fig. 1) by constructing a dam which partially blocks the flow diverting it eastwards (Fig. 9A) into an open channel which traverses the hillside at a low gradient (Fig. 9B) and makes its way into the next valley to the east, to the scattered settlements (which are known as Debring) along the main Manali-Leh highway.

Fig. 9 here

To date no information about the history, purpose, success or future of this scheme has been found. However, there was field evidence to suggest that the channel (which is cut into unconsolidated sands and gravels) has breached in a least two places between 1-2 km from the Zara river. Large gullies were observed running downslope from the channel and in some places they had been filled in to allow the vehicular track, by which the upper valley may be accessed, to be driven.

Conclusions

This 18 day study of the Zara river during the summer melt season has shown that Q ranged between 0.4 and 5.3 m^3/s, and the mean for the period was 1.2 m^3/s, thus maintaining a reliable water supply for this arid, high altitude region. SSC measured in 63 manual samples ranged from 5 to 92 mg/L, and the mean SSC was 17 mg/L. The SSCs are low on a global scale, and particularly when compared to other studies from the monsoon affected regions of the Himalayas. A detailed examination of Q and SSC hysteresis and sediment exhaustion revealed switches in suspended sediment availability during the study period which may be associated with snowmelt and freeze-thaw processes on the surrounding mountainsides and glaciers generating sediment which was then transported downstream by snow meltwater. Thus study has confirmed that the Zara River at this location provides a reliable discharge in August with a relatively low suspended sediment load.

References

Chow, V.T., Maidment, D.R. & Mays, L.W. (1988) *Applied Hydrology*. McGraw-Hill, New York, USA.

Dooge, J.C. (1959) A general theory of the unit hydrograph. *J. Geophys. Res*. **64**(2), 241-256.

Bandyopadhyay, J., Kraemer, D., Kattelmann, R. & Kundzewicz, Z. W. (1997). *Highland waters: A resource of global significance*, in: Mountains of the world: A global priority, edited by: Messerli, B., and Ives, J., Parthenon, New York, 131–155.

Barnett, T. P., Adam, J. C. &Lettenmaier, D. P. (2005) Potential impacts of a warming climate on water availability in snow-dominated regions. *Nature* 438(17), 303–309.

Dyhrenfurth, G. O. (2011) *To the Third Pole-The History of the High Himalaya*. Read Books.

Haritashya, U. K., Singh, P., Kumar, N., & Gupta, R. P. (2006) Suspended sediment from the Gangotri Glacier: Quantification, variability and associations with discharge and air temperature. *Journal of Hydrology,* 321(1), 116-130.

Hasnain, S.I. (1992) Glacio-fluvial sediment transfer from Chhota-Shirgri Glacier, Lahul-Spiti Valley, India. (In: International Symposium on Hydrology of Mountainous Areas. Proceedings. Simla, India, 273-284.)

Hasnain, S.I., Subramanian, V. & Dhanpal, K. (1989) Chemical characteristics and suspended sediment load of meltwaters from a Himalayan glacier in India. *Journal of Hydrology*, 106 (991-2), 99-108.

Hasnain, S. I., & Thayyen, R. J. (1999) Discharge and suspended-sediment concentration of meltwaters, draining from the Dokriani glacier, Garhwal Himalaya, India. *Journal of Hydrology*, 218(3), 191-198.

Herschey, R.W.E. (1978) *Hydrometry, Principles and Practices*. Chichester, Wiley. 511pp.

Hobley, D.E., Sinclair, H.D. & Mudd, S.M. (2012) Reconstruction of a major storm event from its geomorphic signature: The Ladakh floods, 6 August 2010. *Geology,* 40(6), 483-486.

Immerzeel, W.W., Droogers, P., de Jong, S.M. & Bierkens, M.F.P. (2009) Large-scale monitoring of snow cover and runoff simulation in Himalayan river basins using remote sensing. *Remote Sensing of Environment,* 113, 40–49.

Immerzeel, W.W., van Beek, L. P. H. & Bierkens, M. F.P. (2010) Climate change will affect the Asian water towers. *Science,* 328, 1382–1385.

India Meteorological Department (2010) Cloud burst over Leh (Jammu & Kashmir): India Meteorological Department Public report, www.imd.gov.in/doc/cloud-burst-over-leh.pdf, 4 p.

Intergovernmental Panel on Climate Change (2007) Climate change 2007-the physical science basis: Working group I contribution to the fourth assessment report of the IPCC (Vol. 4). Cambridge University Press.

Lana-Renault, N., Alvera, B. & García-Ruiz, J.M. (2011) Runoff and sediment transport during the snowmelt period in a Mediterranean high-mountain catchment. *Arctic, Antarctic, and Alpine Research*, 43(2), 213-222.

Morton, K. (2011). Climate change and security at the third pole. *Survival,* 53(1), 121-132.

Schmidt, S. & Nüsser, M. (2012) Changes of high altitude glaciers from 1969 to 2010 in the trans-himalayan Kang Yatze Massif, Ladakh, northwest India. *Arctic, Antarctic, and Alpine Research*, 44(1), 107-121.

Spate, O.H.K., Learmonth, A.T.A. & Farmer, B.H. (1976) *India, Pakistan and Ceylon* (second revised edition): London, Methuen and Co., Ltd., p. 424–450.

Stott, T.A., Nuttal, A. & Biggs, E. (2014) Observed runoff and suspended sediment dynamics from a minor glacierzied basin in South-West Greenland. *Geografisk Tidsskrift-Danish Journal of Geography,* 114 (2), 93-108.

Thayyen, R. J., & Gergan, J. T. (2010) Role of glaciers in watershed hydrology: a preliminary study of a" Himalayan catchment". *The Cryosphere,* 4(1), 115-128.

Viviroli, D. & Weingartner, R. (2004) The hydrological significance of mountains: from regional to global scale, *Hydrology and Earth System Sciences* 8, 1017–1030.

Viviroli, D., Durr, H. D., Messerli, B., Meybeck, M. & Weingartner, R. (2007) Mountains of the world, water towers for humanity: Typology, mapping, and global significance. *Water Resour. Res.*, 43, W07447, doi:10.1029/2006WR005653.

Walling, D.E. & Fang D (2003). Recent trends in the suspended sediment loads of the world's rivers. *Global and Planetary Change,* 39(1), 111-126.

Figures

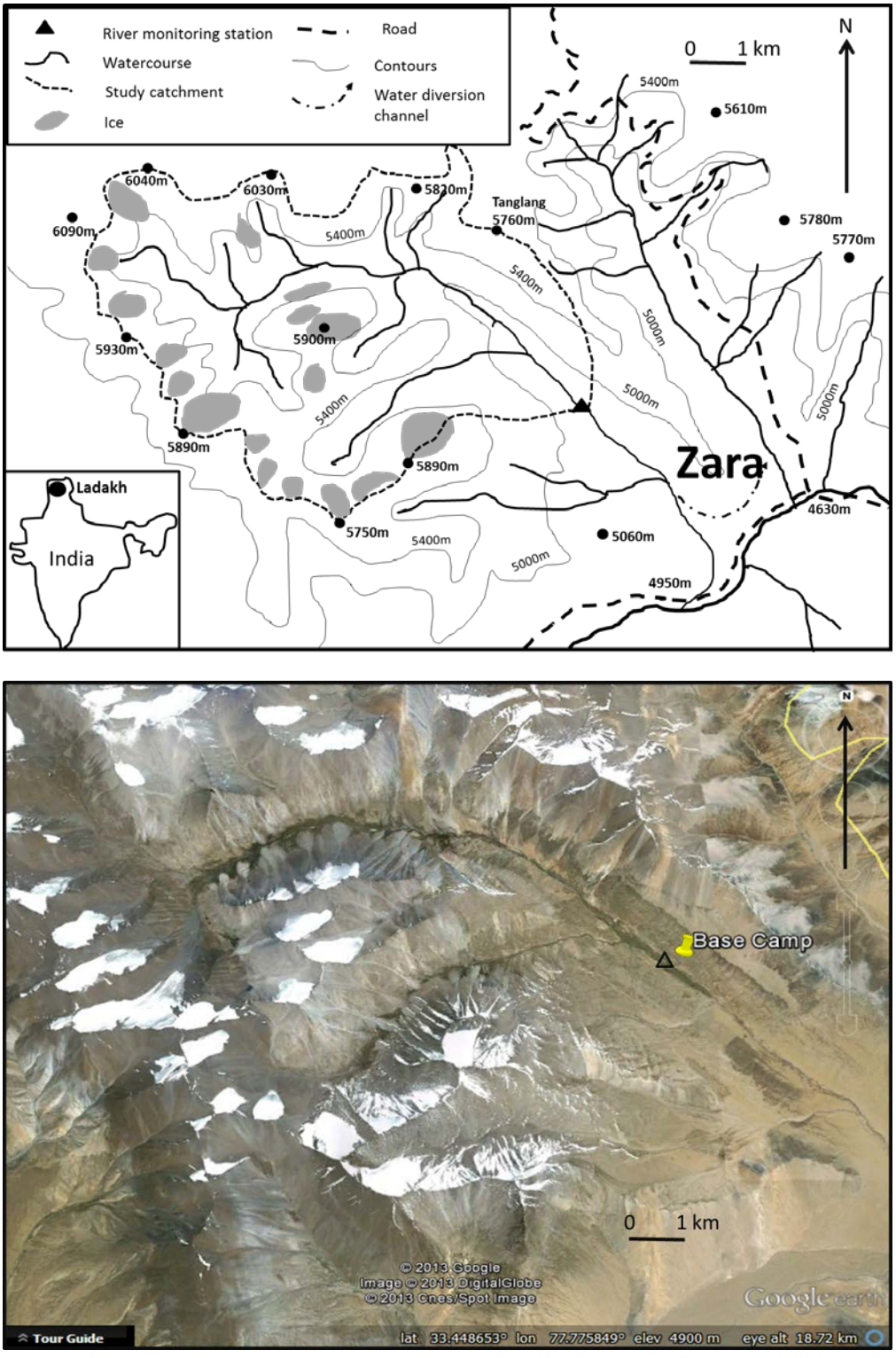

Figure 1: Study location map (Top); Google Earth image (2013) showing location of river monitoring site (Δ)

Fig. 2A: View of glaciers on west side of study catchment. View looking NW. Glaciers are on NE slopes at 5400 – 6000m altitude.

Fig. 2B: View of typical glaciers in study catchment. View looking west. Glacier is on NE slope at 5400 – 5750m altitude.

Fig. 2C: Stage board with pressure transducer. The turbidity sensor is fixed to floating ring and the TinyTag air temperature logger is on the bank (photo: T. Stott).

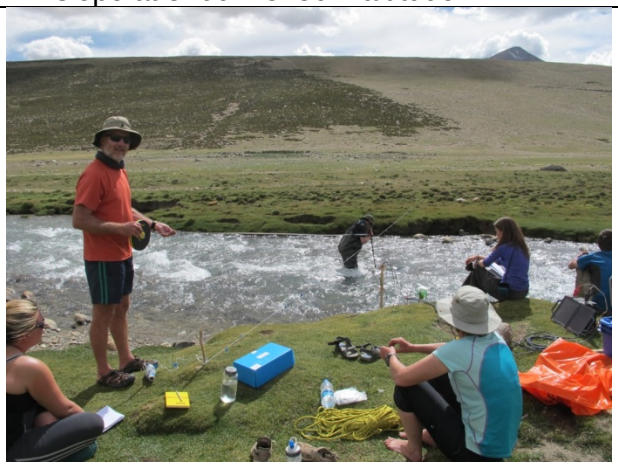

Fig. 2D: Meausuring river discharge using a Braystoke flow meter (photo: H. Souterou).

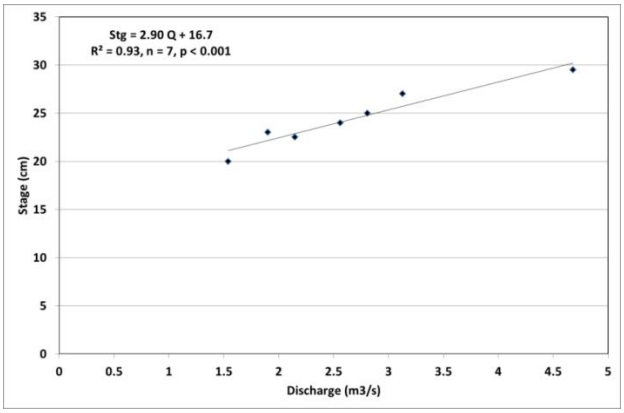

Fig. 3A: Stage v discharge (Q) rating curve, for Zara River, August 2013

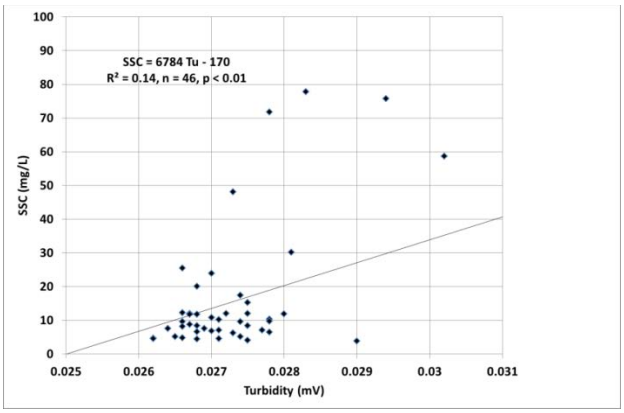

Fig. 3B. Suspended sediment concentration (SSC) v turbidity (Tu) calibration relationship for Zara River, August 2013.

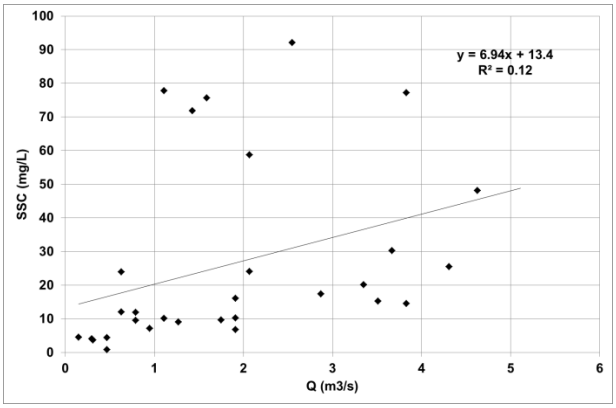

Fig. 3C. Suspended sediment concentration (SSC) v discharge (Q) relationship for Zara River, August 2013.

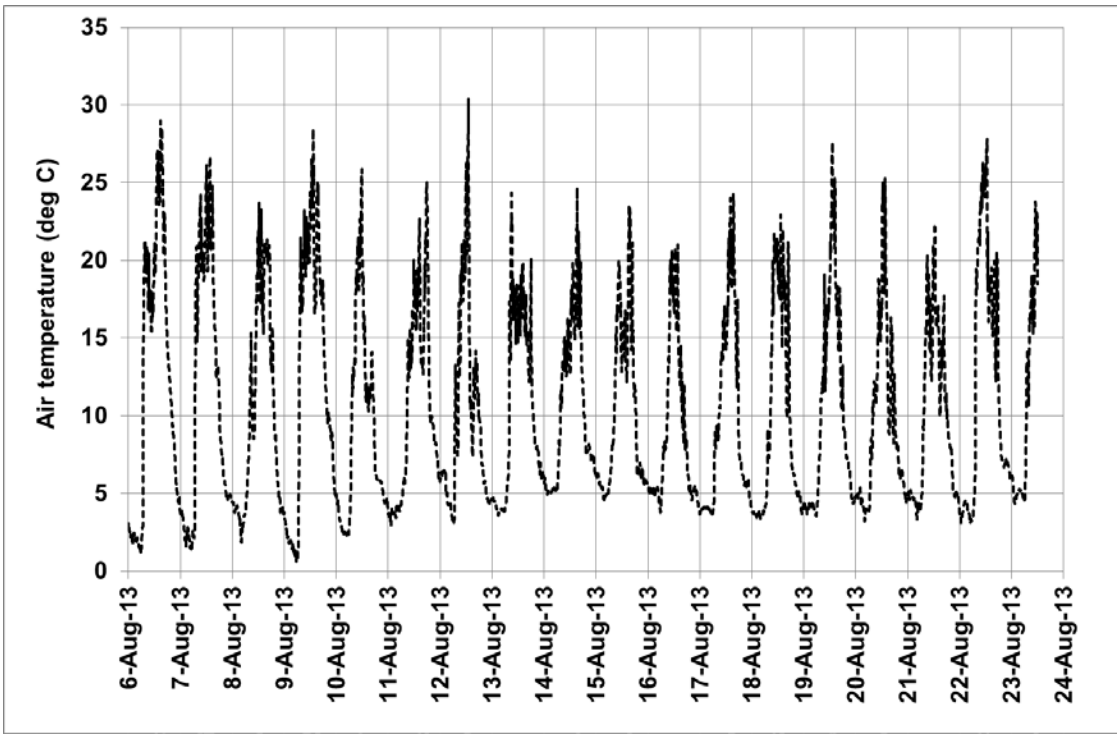

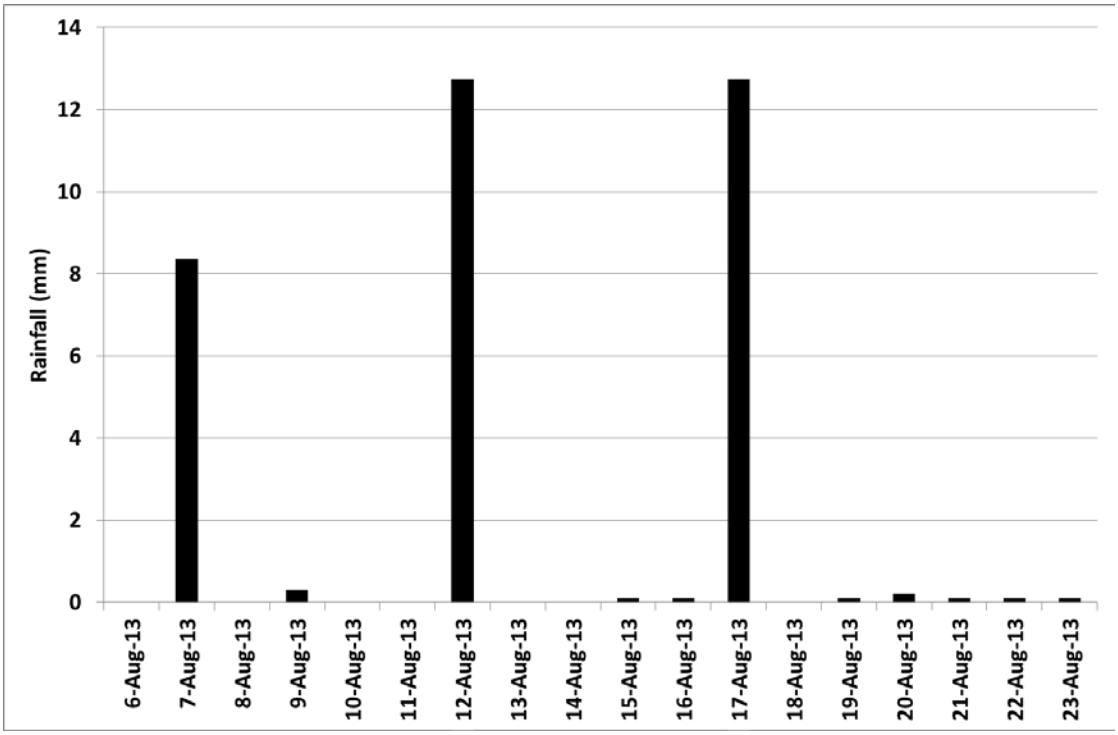

Fig. 4: A. 5-min air temperature record and, B. Daily rainfall during the study period.

A.

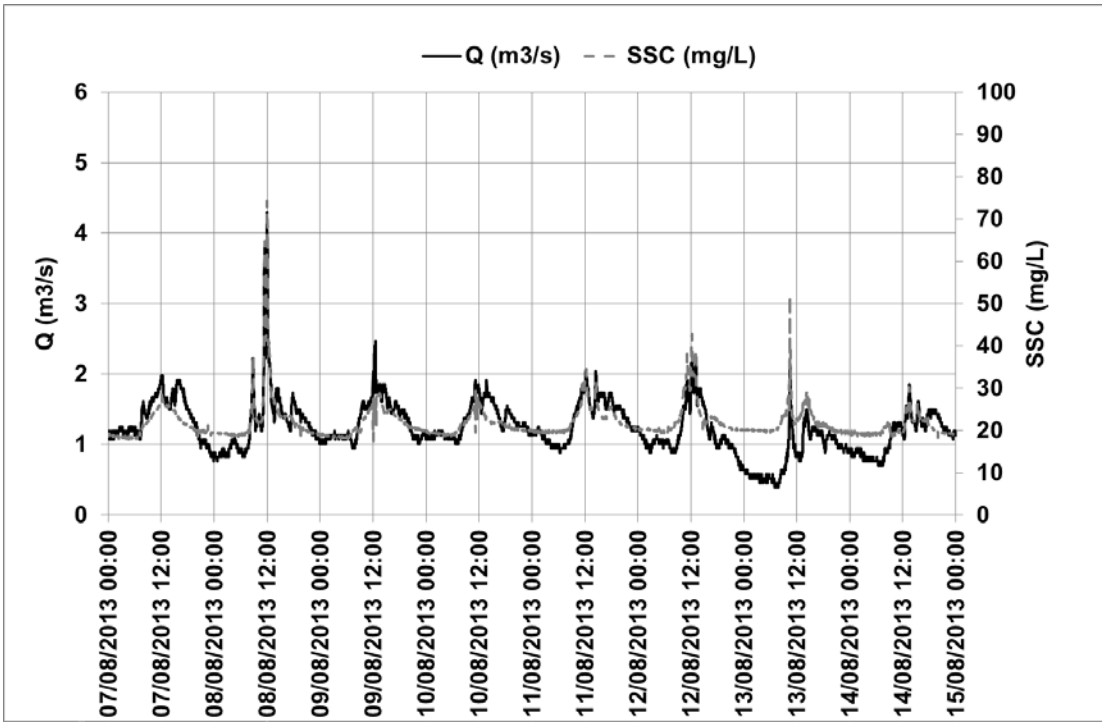

B.

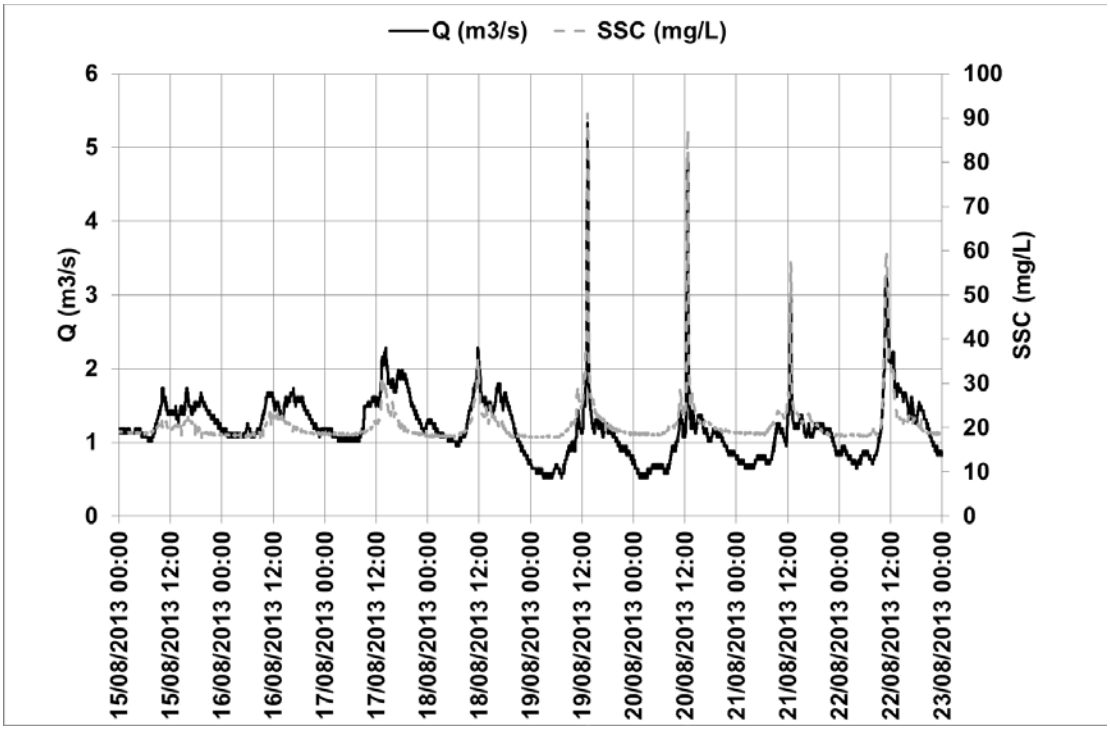

Figure 5: Discharge (Q) and predicted suspended sediment concentration (SSC) time series for Zara river, (A) 7-14 August 2013, (B) 15-22 August 2013.

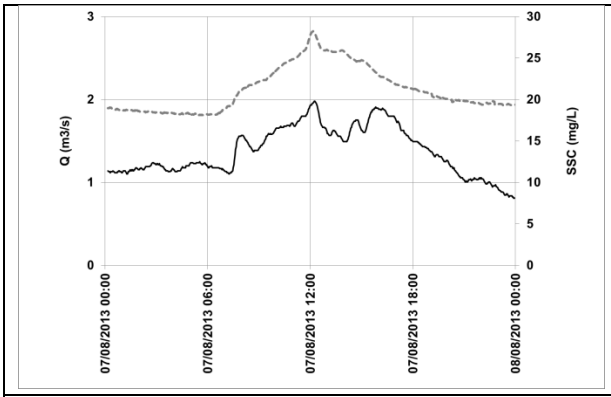

A: Q and SSC time series plot for 7-Aug-13

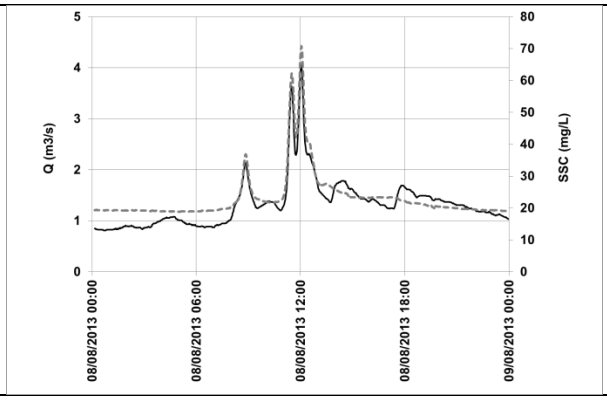

B: Q and SSC time series plot for 8-Aug-13

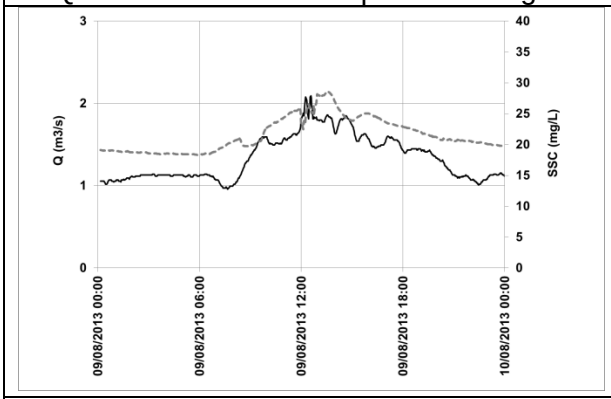

C: Q and SSC time series plot for 9-Aug-13

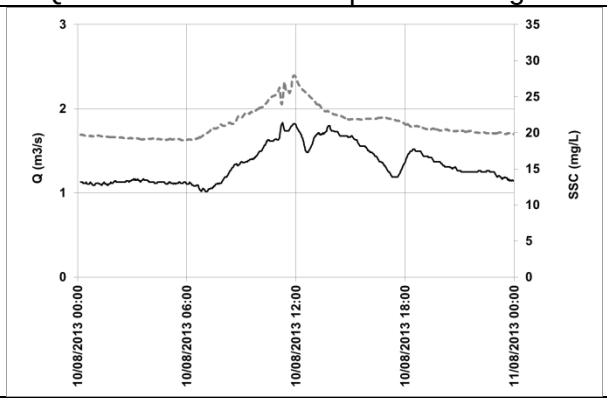

D: Q and SSC time series plot for 10-Aug-13

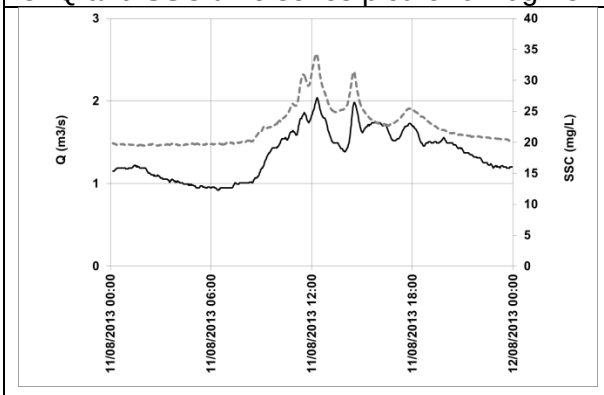

E: Q and SSC time series plot for 11-Aug-13

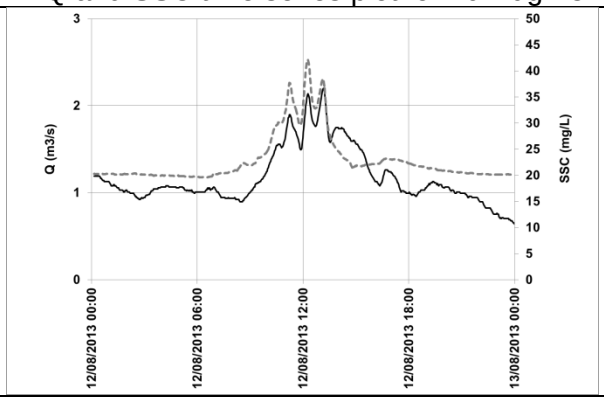

F: Q and SSC time series plot for 12-Aug-13

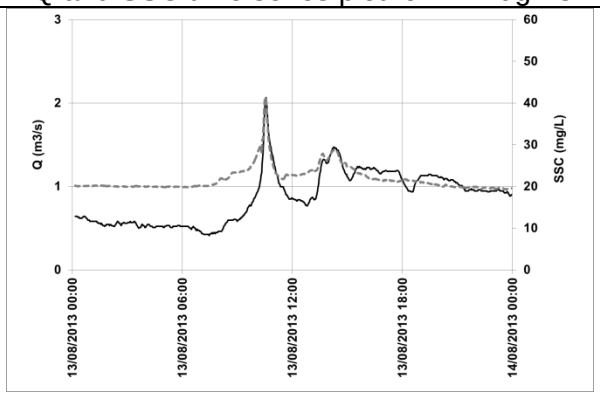

G: Q and SSC time series plot for 13-Aug-13

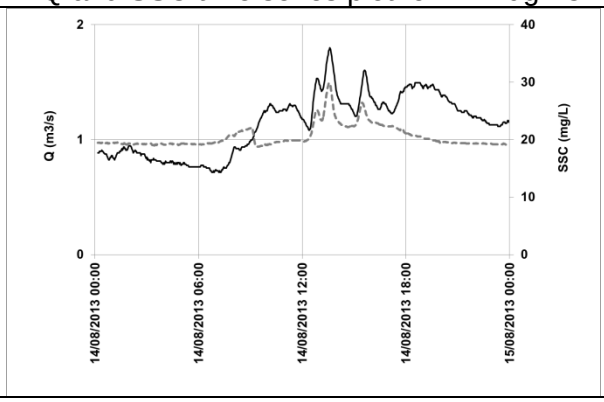

H: Q and SSC time series plot for 14-Aug-13

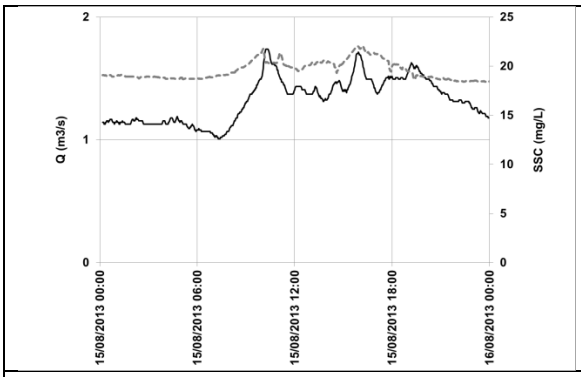

I: Q and SSC time series plot for 15-Aug-13

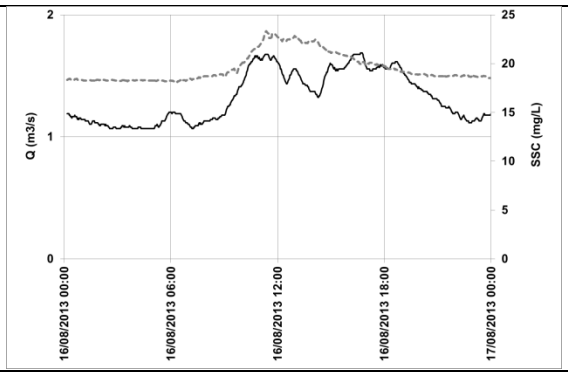

J: Q and SSC time series plot for 16-Aug-13

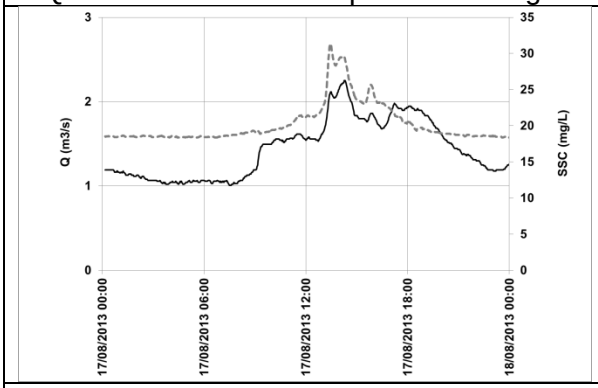

K: Q and SSC time series plot for 17-Aug-13

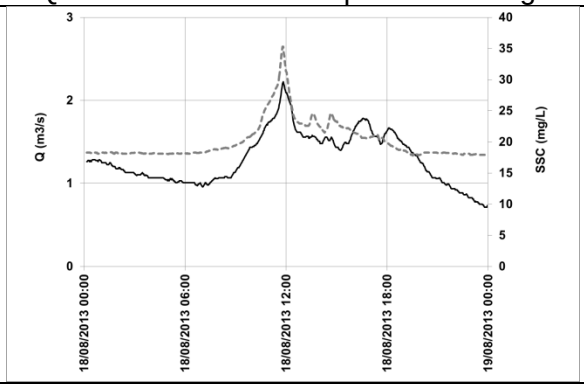

L: Q and SSC time series plot for 18-Aug-13

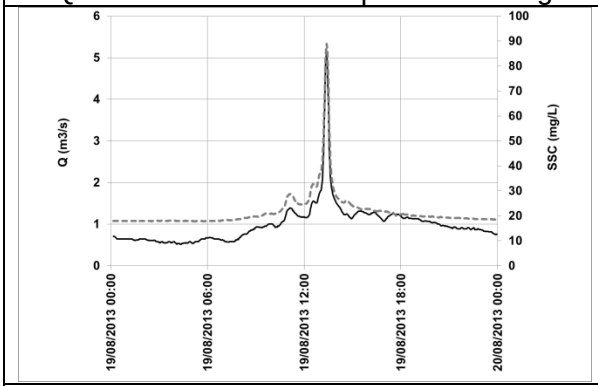

M: Q and SSC time series plot for 19-Aug-13

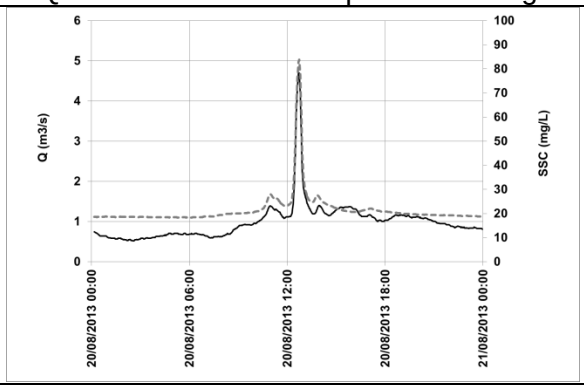

N: Q and SSC time series plot for 20-Aug-13

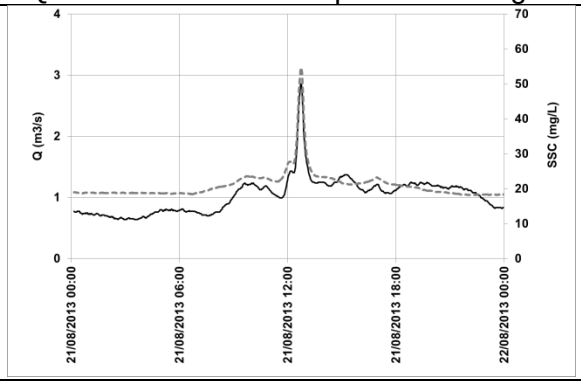

O: Q and SSC time series plot for 21-Aug-13

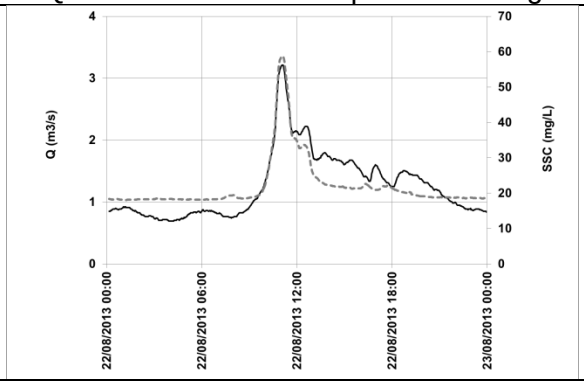

P: Q and SSC time series plot for 22-Aug-13

Fig.6: Discharge (Q) and suspended sediment concentration (SSC) time series plot for 7-22 August 2013 in the Zara River, Ladakh. (NB: Bold black lines = Q; grey dotted lines = SSC).

Fig. 7:

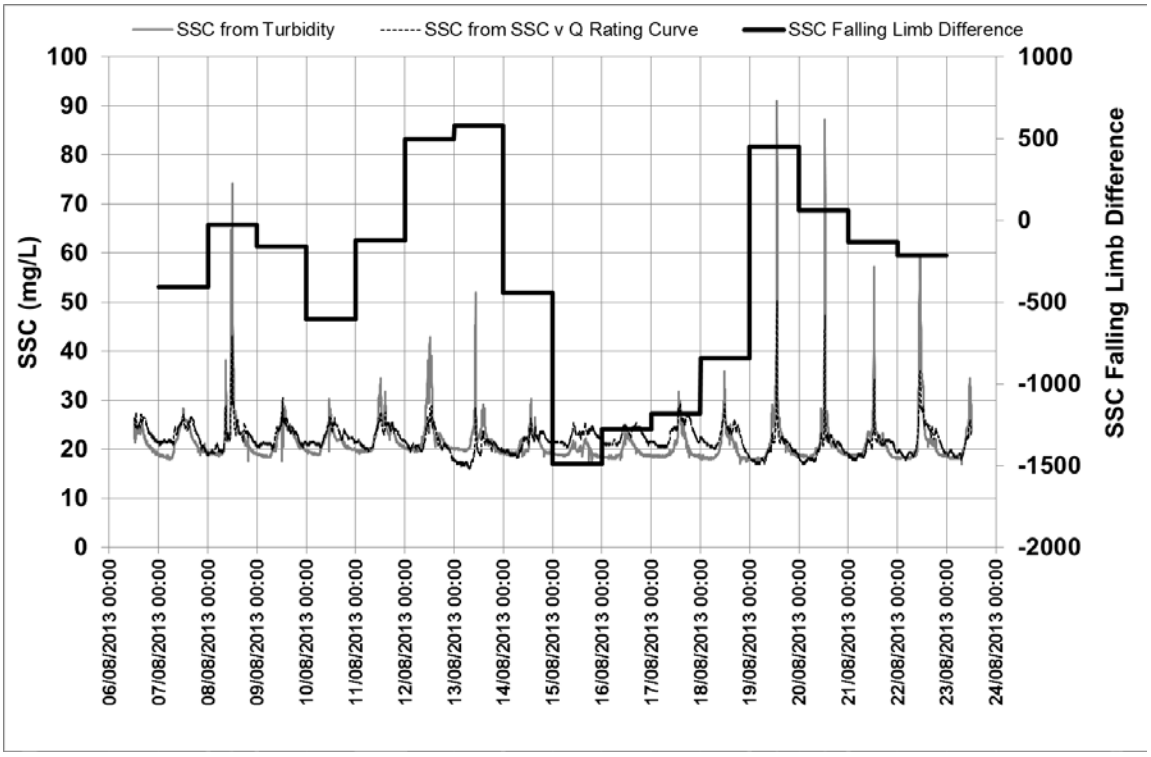
SSC from Turbidity
SSC from SSC v Q Rating Curve
SSC Falling Limb Difference
SSC (mg/L)
SSC Falling Limb Difference
100
90
80
70
60
50
40
30
20
10
0
1000
500
0
-500
-1000
-1500
-2000
06/08/2013 00:00
07/08/2013 00:00
08/08/2013 00:00
09/08/2013 00:00
10/08/2013 00:00
11/08/2013 00:00
12/08/2013 00:00
13/08/2013 00:00
14/08/2013 00:00
15/08/2013 00:00
16/08/2013 00:00
17/08/2013 00:00
18/08/2013 00:00
19/08/2013 00:00
20/08/2013 00:00
21/08/2013 00:00
22/08/2013 00:00
23/08/2013 00:00
24/08/2013 00:00

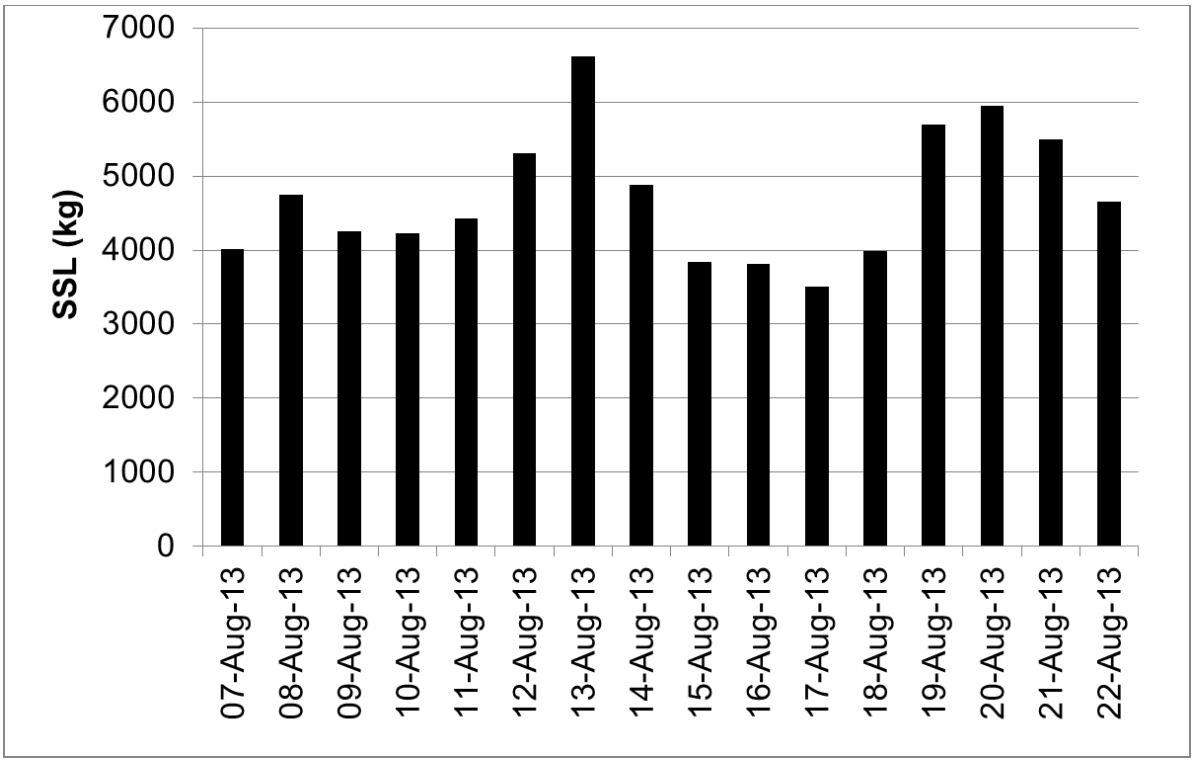

Figure 8: Daily suspended sediment load for Zara River 7-22 August 2013.

Fig. 9A: Water abstraction dam on Zara river 2 km downstream from monitoring site (photo: T. Stott).

Fig. 9B: Excavated channel intended to carry water from the Zara river to Debring in the next valley to the east (photo: T. Stott).

Table 1: Analysis of lag times for Zara River, 7-22 August 2013.

Date	Q_{peak} Time	Q_{peak}	Peak T_{air} Time	Peak T_{air}	Q_{peak} to Peak T_{air} Lag Time	SSC_{peak} Time	SSC_{peak}	Q_{peak} to SSC_{peak} Lag time	Hysteresis ?	Rainfall
07-Aug-13	11:59:00	1.98	13:40:00	27.00	**+01:41:00**	11:23:00	27.50	-00:36:00	Anticlockwise	8.4
08-Aug-13	11:57:00	4.23	12:25:00	23.7	**+00:28:00**	11:59:00	74.3	**+00:02:00**	Clockwise	0.0
09-Aug-13	12:31:00	2.47	13:25:00	28.5	**+00:54:00**	12:58:00	27.9	**+00:27:00**	Clockwise	0.3
10-Aug-13	11:09:00	1.92	11:45:00	25.9	**+00:36:00**	11:15:00	30.2	**+00:06:00**	Clockwise	0.0
11-Aug-13	12:17:00	2.04	17:50:00	24.9	**+05:33:00**	12:13:00	34.5	-00:04:00	Anticlockwise	0.0
12-Aug-13	13:03:00	2.22	13:05:00	30.4	**+00:02:00**	12:11:00	42.7	-00:52:00	Anticlockwise	12.7
13-Aug-13	10:25:00	2.16	08:55:00	24.4	-01:30:00	10:25:00	51.9	00:00:00	None	0.0
14-Aug-13	13:31:00	1.86	15:15:00	24.7	**+01:44:00**	13:31:00	30.2	00:00:00	None	0.0
15-Aug-13	10:05:00	1.74	15:40:00	23.3	**+05:35:00**	15:53:00	21.8	**+05:48:00**	Clockwise	0.1
16-Aug-13	16:39:00	1.74	13:50:00	21	-02:49:00	12:17:00	23.2	-04:22:00	Anticlockwise	0.1
17-Aug-13	14:11:00	2.29	15:35:00	24.3	**+01:24:00**	13:19:00	21.6	-00:52:00	Anticlockwise	12.7
18-Aug-13	11:45:00	2.29	13:25:00	22.9	**+01:40:00**	11:41:00	35.7	-00:04:00	Anticlockwise	0.0
19-Aug-13	13:17:00	5.33	13:10:00	27.6	-00:07:00	13:21:00	89.9	**+00:04:00**	Clockwise	0.1
20-Aug-13	12:39:00	4.9	13:40:00	25.3	**+01:01:00**	12:41:00	87.2	**+00:02:00**	Clockwise	0.2
21-Aug-13	12:41:00	3.02	12:25:00	22.2	-00:16:00	12:41:00	57.4	00:00:00	None	0.1
22-Aug-13	10:59:00	3.26	12:35:00	27.8	**+01:36:00**	11:05:00	58.9	**+00:06:00**	Clockwise	0.1
MAX	16:39:00	5.33	17:50:00	30.40	**+05:35:00**	15:53:00	89.90	**+05:48:00**		12.7
MIN	10:05:00	1.74	08:55:00	21.00	00:02:00	10:25:00	21.60	00:00:00		0.0
MEAN	12:26:45	2.72	13:32:30	25.24	**+01:41:00**	12:25:49	44.68	**+00:50:19**		2.2